Mechanistic Understanding of Degradation in Bioerodible Polymers for Drug Delivery

Domenico Larobina and Giuseppe Mensitieri
Dept. of Materials and Production Engineering, University of Naples "Federico II", Naples, Italy 80125

Matt J. Kipper and Balaji Narasimhan
Dept. of Chemical Engineering, Iowa State University, Ames, IA 50011

A new model was developed to understand the mechanism of erosion in bioerodible polymers, which is essential to accurately predict drug release and precisely design controlled release devices. This model takes into account the phenomenon of microphase separation observed for polyanhydrides of certain copolymer compositions, and assumes that erosion is dominated by degradation and, thus, in a system with a fast eroding and a slow eroding species, two rate constants — one for each species — essentially control the evolution of the polymer microstructure. Expressions were derived for the fraction of each monomer released, as well as for the porosity in the system. A partition coefficient accounts for thermodynamic partitioning of a drug into the microdomains. The solutions of the model equations were fitted to experimental data on monomer release kinetics from two polyanhydride systems to obtain the erosion rate constants. Drug release kinetics experiments are compared to the model solution for drug release, and the partition coefficient of the drug is obtained from the fits. The comparisons to the data are promising, while pointing out the limitations of the model. The model does not account for oligomer formation prior to monomer release or for the dependence of the rate constants on parameters such as the degree of crystallinity, the local pH, and the polymer molecular weight.

Introduction

The use of biodegradable polymers as carriers for controlled release systems has been the object of research over the past two decades due to their advantages over other competing systems. The biodegradable structure of the polymer obviates the need to surgically remove the device. Biocompatibility of the degradation products has also been established. For example, the FDA has approved the use of the copolymer, poly[1,3-bis(*p*-carboxyphenoxy)propane-*co*-sebacic anhydride], p(CPP-SA) 20:80, for human use, and the delivery of anti-cancer proteins has been reported (Dang et al., 1996).

For clarity, it is important to distinguish between the terms "degradation" and "erosion". The term "degradation" refers to the chain scission process by which polymer chains are cleaved into oligomer or monomer units. The term "erosion" refers to mass loss from the bulk polymer. In other words, erosion could be considered as the sum of several elementary processes, one of which is degradation.

The pioneering work of Langer, Mathiowitz, and coworkers (Chasin et al., 1988; Domb and Langer, 1987; Goepferich et al., 1995; Leong et al., 1986, 1985; Mathiowitz et al., 1990a,b, 1988; Mathiowitz and Langer, 1987; Shieh et al., 1994; Tamada and Langer, 1992) has established the potential of biodegradable polyanhydrides based on aromatic and aliphatic dicarboxylic acids as carriers for therapeutic compounds. This class of polyanhydrides consists of a backbone of monomeric carboxylic diacids joined by anhydride linkages; these bonds are hydrolyzed upon exposure to an aqueous environment, forming water-soluble monomeric degradation products. In spite of the hydrophilicity of the characteristic anhydride functional group, the presence of aromatic and aliphatic groups in the monomer confers a high hydrophobicity to the polymer. As a consequence, water is

Correspondence concerning this article should be addressed to B. Narasimhan.

prevented from penetrating into the bulk of the polymeric device causing the erosion process to occur on the surface of the device (Goepferich, 1996a,b). This is in contrast to "bulk-erodible" polymers such as poly(lactic acid), poly(glycolic acid), and their copolymers, in which water penetrates into the bulk of the polymer (Langer, 1990; Peppas and Langer, 1994). The polyanhydride system is extremely versatile due to the differences in the homopolymer erosion rates; in fact, by simply employing different comonomer ratios, the erosion times can be varied from a few weeks to a few years (Leong et al., 1985).

Several studies report *in vitro* erosion of copolymeric polyanhydrides. Some of the earlier work with this system reported only *total* mass loss (Chasin et al., 1988; Leong et al., 1985; Mathiowitz et al., 1990a, 1988; Mathiowitz and Langer, 1987; Shieh et al., 1994; Tamada and Langer, 1992); but, more recently, individual monomer release has been reported because this information provides a more detailed view of the mechanism of degradation (Shen et al., 2002; Tamada and Langer, 1990). Recent studies conducted by our group have shown that depending on the copolymer composition, the system based on sebacic anhydride (SA) and 1,6-bis(*p*-carboxyphenoxy)hexane (CPH) (see Figure 1) undergoes microphase separation (Shen et al., 2001). For compositions that contain one component in excess of ~ 80 mol%, we have shown earlier, using a combination of nuclear magnetic resonance (NMR), atomic force microscopy (AFM), differential scanning calorimetry (DSC), and wide angle X-ray diffraction (WAXD), that the polymer microstructure exhibits microphase separation. The presence of microphase separation in such systems is due to a combination of two factors. First, the reactivity ratio of the co-monomers, SA and CPH, are both close to unity (Ron et al., 1991; Shen et al., 2002), and, hence, if there is an excess of the SA component, SA-SA bonds are more abundant than SA-CPH or CPH-CPH bonds. Second, the relative hydrophobicity of the two co-monomers is different (manifested by their vastly differing degradation rates), and, thus, in situations where, for example, SA-SA bonds are numerous, the fewer CPH moieties thermodynamically prefer to form "microdomains" within a matrix of SA. Thus, on a microscopic scale, two equilibrium phases are

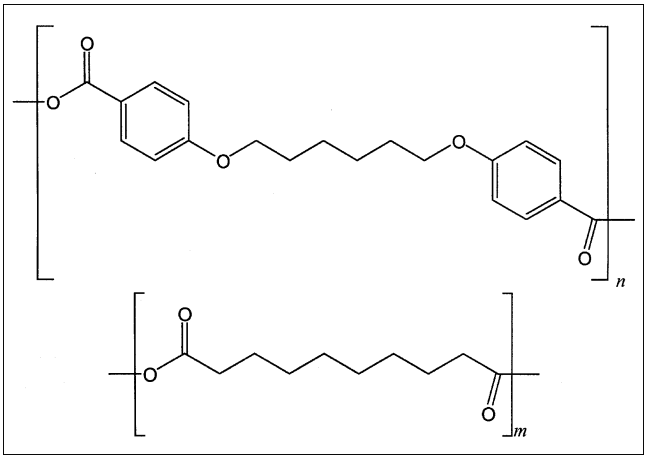

Figure 1. Chemical structures of CPH (top) and SA (bottom) repeat units.

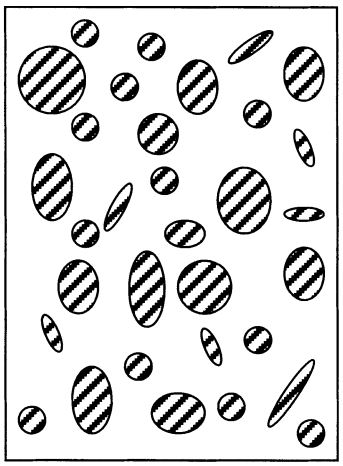

Figure 2. Microphase separation in polyanhydrides.

formed with each phase containing predominantly one constituent. This structure is represented in Figure 2.

Furthermore, it can be argued that if there is microphase separation in polyanhydrides of a certain copolymer composition, drugs loaded into such polymers may thermodynamically partition into one phase or the other, depending on the compatibility of the drug with the constituent monomers. Careful examination of the literature on *in vitro* drug release from polyanhydrides of specific compositions reveals that drug release profiles (Chasin et al., 1988; Mathiowitz and Langer, 1987) do *not* match polymer erosion profiles over the *entire duration* of release. In fact, drug release profiles match individual monomer release profiles depending on their compatibility to the monomer phase. Thus, for example, the release of *p*-nitroaniline (PNA), which is mainly dissolved in the slowly eroding phase (CPP or CPH), mimics the erosion profile of that phase once the fast eroding phase (SA) is dissolved (Shen et al., 2002). Qualitatively similar inferences can be drawn by observation of release data of other compounds loaded into copolymers of the same family (Chasin et al., 1988; Chickering et al., 1996; Kuntz and Saltzman, 1997; Leong et al., 1985; Mathiowitz et al., 1988, 1990a, 1992; Mathiowitz and Langer, 1987; Olivi et al., 1996; Park et al., 1997, 1998; Shieh et al., 1994).

A fundamental understanding of the mechanism of degradation is essential to accurately predict drug release and precisely design controlled release devices. The development of a preliminary model that accounts for both microphase separation and drug partitioning is the main subject of this article. The next section provides a brief summary of current models that describe polymer degradation and drug release. The following two sections present the assumptions and the salient features of the new model, and discuss the estimation of key model parameters from comparisons to experimental data, limitations of the model, and suggestions for improvements. The last section highlights the main conclusions of this work.

Previous Models

One of the first mathematical models describing the diffusive release of a drug from a polymeric device undergoing surface erosion was developed by Thombre and Himmelstein

(1984). They assumed that the erosion front moves with a zero-order velocity and that Fickian diffusion occurs in the noneroded zone under pseudo-steady-state conditions. Consequently, two boundaries simultaneously move from the surface of the device to its center. This analysis, which was also extended to similar devices with a secondary membrane, fundamentally aimed to characterize the concentration profile of the drug inside the device and was able to predict fractional mass loss based on the drug concentration profile within the polymer. The same authors (Thombre and Himmelstein, 1985) have developed another model, which accounts for diffusion of all the species involved in the process. In addition, autocatalytic reaction of the polymer during degradation is taken into account. The system studied was made of a poly(orthoester) matrix in which an acid anhydride and a bioactive agent are uniformly distributed. The presence of the acid anhydride catalyzed degradation of the polymer matrix according to an elementary three-step reaction, which ultimately hydrolyzed the polymer.

A different approach to understand the mechanism of degradation was proposed by Zygourakis (Zygourakis, 1990; Zygourakis and Markenscoff, 1996). He used the cellular automata method, first discretizing the system into cells, each one defined as either a polymer or a drug. Furthermore, each type of cell was characterized by a time constant for dissolution upon exposure to solvent. Dissolution time steps were then iterated to compute the temporal evolution of the erosion front and drug release. The resulting profiles showed almost linear fractional mass release profiles in contrast with the sigmoidal release that many experimental data show (Chasin et al., 1988; Mathiowitz et al., 1988; Park et al., 1998; Shen et al., 2002; Shieh et al., 1994).

Goepferich and Langer (1993) developed a stochastic model using Monte Carlo methods that consider the presence of multiple phases in the polymer matrix, which was otherwise similar to the cellular automata approach of Zygourakis. An important similarity between the models of Zygourakis and Goepferich and Langer is that erosion is considered an elementary process. The models differ in that Goepferich and Langer assumed finite probabilities for each erosion event, instead of assigning a constant velocity for erosion, and did not consider drug loading. Their model was applied to polyanhydrides using two types of polymer cells with different characteristic erosion times corresponding to crystalline and amorphous zones. The time constants were evaluated by fitting to experimental *in vitro* erosion data, and not explicitly correlated to physical processes such as hydrolysis, dissolution, and subsequent diffusion. Goepferich and Langer (1995) further developed this model to include monomer diffusion through the resulting porous network.

More recently, a quantitative model was developed by Batycky et al. (1997) to predict mass loss, molecular weight change, and macromolecular drug release as a function of time for the case of bulk eroding microspheres. In this model, the two mechanisms of chemical degradation, that is, random chain scission and end scission, were combined to obtain a more accurate prediction of the observed mass and molecular weight evolution. Two (coupled) drug release processes are accounted for: desorption from the surface in contact with the buffer solution, and Fickian diffusion through mesopores. The desorption leads to a burst release from the initially exposed surface in contact with the buffer solution. A subsequent lag time in the drug release is attributed to the induction time associated with the growth of micropores and their coalescence to form mesopores sufficiently large for release of additional macromolecular drug.

It is worthwhile to note that all the models described above were developed for polymers with homogenous composition; thus, the drug is uniformly distributed throughout the polymer matrix and there is no thermodynamic partitioning. One model that does account for partitioning was developed by Varelas et al. (1995a,b). In this model, the drug is encapsulated in a polymeric dispersed phase and diffuses through a continuous phase. The continuous phase is a hydrogel in which the drug is only slightly soluble. Thus, the dispersed phase acts as a reservoir, a pseudo-steady state is obtained during release, and release is zero-order. The device is not bioerodible.

The existence of microphase separation in polymers and consequent partitioning of drugs into the microdomains necessitates the development of new models that incorporate these phenomena into the analysis. This is the main goal of the current work. In addition, physical significance will be assigned to model parameters by linking them to elementary physical processes. Furthermore, the parameters will be compared to independent experiments to verify the validity of the assumptions intrinsic to the model.

Model Development

In general, polymer erosion is a complex phenomenon that depends on many factors such as: polymer degradation, polymer chemistry and composition, crystallinity, hydrophobicity, polymer molecular weight, and diffusivity of monomers and oligomers. Each of these factors plays a different role in determining the rate of erosion. Schematically, the erosion process is composed of the following elementary steps:

(1) *Water Ingress*. Initially, the polymeric device is exposed to an aqueous buffer solution, which leads to water ingress. Two kinds of degradation mechanisms can be distinguished: bulk and surface, depending on the polymer hydrophobicity.

(2) *Chemical Degradation*. The water randomly breaks the chemical bonds in the polymer and produces the constituent monomers and oligomers.

(3) *Dissolution*. Finally, the monomers dissolve in the buffer and diffuse through the device into the bulk.

Thus, the erosion process could be viewed as the sum of different elementary processes, each characterized by a time constant. The analysis of these processes with the associated time constants allows us to discern which ones might be rate limiting and, consequently, which could be ignored in order to achieve a simplified model.

A new model has been developed that describes the surface erosion of biodegradable polymers, which are comprised of microphase-separated domains. We have chosen the copolymeric polyanhydride system based on SA and CPP (or CPH) as a starting point. In this system, microphase separation occurs when one component of the copolymer is present in excess (that is, > 80 mol%) (Shen et al., 2001).

We have recently performed experiments (Shen et al., 2002) in which we analyzed the release of each of the constituent monomers of the CPH-SA system, in addition to the overall

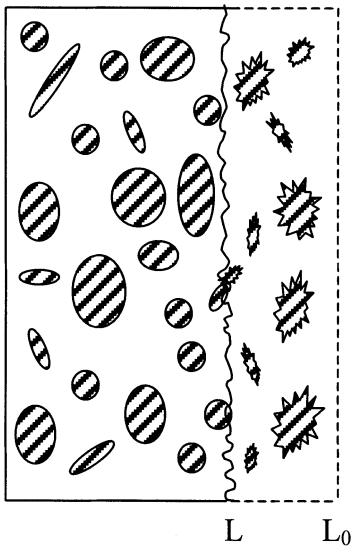

Figure 3. Polyanhydride tablet of half-thickness L_0, the noneroded core, and the progression of the eroding zone, represented by the broken line $L(t)$.

polymer erosion. The system consisted of a tablet whose thickness was small compared to the diameter (aspect ratio ~ 10), so that one-dimensional (1-D) transport could be assumed. The coordinate system of choice has its origin at the center of the tablet of total thickness $2L_0$. Symmetry enables the development of model equations for $0 \le x \le L_0$. From these experiments, we know that:

(1) The thickness of the matrices prepared from these copolymers does not change for several days during erosion;

(2) The erosion front that separates the eroding and the noneroded zones always moves parallel to the polymer surface that is exposed to the buffer solution (see Figure 3).

(3) The hydrophobic nature of the copolymers does not allow water to penetrate into the core of the tablet; thus, degradation occurs on the surface.

Additionally, the rate of scission of the bonds for the copolymer p(SA-CPP) was recently evaluated using NMR spectroscopy (Heatley et al., 1998; McCann et al., 1999). The results showed that the degradation rate of the SA-SA bond is of the same order of magnitude as that of the SA-CPP bond and two orders of magnitude less than that of the CPP-CPP bond.

Starting from these considerations, it is clear that the reaction/transport process that takes place within the copolymer is essentially governed by two different time constants, one associated with SA erosion ("fast" erosion zone) and the other with CPP or CPH erosion ("slow" erosion zone). For the sake of simplicity, we will refer to the fast eroding species (SA monomer) as A and the slowly eroding species (CPH or CPP monomer) as B.

As reported previously (Goepferich, 1996a,b; Goepferich et al., 1995), after a short period of time referred to as the "induction period", which is attributed to several phenomena (the most important of which is the initial appearance of the monomer), the erosion of A proceeds at constant velocity, *independent* of the A concentration outside the tablet. This indicates that the diffusion rate of A through and the dissolution rate of A within the eroding zone of the tablet may play a minor role in determining the overall erosion kinetics. From these observations, we assume as a first approximation that the erosion process of each constituent of the copolymer is controlled by the degradation of the corresponding monomer-monomer bond. We note, however, that Goepferich and Langer also showed considerable buildup of monomer crystals near the surface of the polymer during erosion, indicating that polymer degradation and monomer dissolution may not occur simultaneously (Goepferich and Langer, 1993). If the drug release kinetics can be well correlated to monomer release, the need to treat monomer crystallization and dissolution in the foregoing model is obviated. Thus, these effects can be essentially lumped into an erosion rate constant. The erosion of species A can be described by a surface zero-order reaction

$$\frac{dm_A}{dt} = M_A S' \phi_{A0} (1-p) k'_A \tag{1}$$

In Eq. 1, m_A is the mass of species A lost from the tablet; M_A is the molecular weight of species A; S' is the effective surface area in contact with the buffer solution; ϕ_{A0} is the surface fraction of A domains; k'_A is the molar average surface erosion rate; and p is the mole fraction of B present in the A domains. The erosion rate constant k'_A is assumed to be constant, although slow diffusion of polymer degradation products may have a considerable effect on the local pH as reported by Mader et al. (1997), accelerating erosion.

Previous studies using atomic force microscopy (Shen et al., 2001) (AFM) are in agreement with the result predicted from theoretical calculations of the phase diagram that a small fraction of the constituent of the dispersed phase may be present within the matrix phase. In the absence of experimental data, the parameter ϕ_{A0} can be estimated as the volume fraction of the A domains and p can be estimated by considering the probability of finding an A-B bond in a randomly distributed medium of A-A, A-B, and B-B bonds.

In order to model the polymer surface, we hypothesize that S' is the product of the cross-sectional area S and a constant term r that accounts for the roughness of the surface. In general, the surface roughness changes continuously during erosion so the assumption is only valid in the limit of short induction periods and for pseudo-steady-state conditions. Since S' is written as Sr and the term r is independent of the geometrical configuration of the tablet, it can be combined with the k'_A constant, leading to a single constant k_A that contains all the information about the erosion process (that is, $k_A = k'_A r$). Thus, we can define the molar average surface erosion rate k_A as the rate at which the erosion front L is moving inside the tablet. Hence, we have

$$k_A = \left[(1-p)\frac{\rho_A}{M_A} + p\frac{\rho_B}{M_B} \right] \frac{dL}{dt} = \bar{\rho}\frac{dL}{dt} \tag{2}$$

Here, $\bar{\rho}$ is the average molar density of the A domains, and ρ_A and ρ_B are the mass densities of A and B, respectively. (The units of k_A are moles per area per time.) By integration of Eq. 2 with the condition that at $t = 0$, $L = L_0$, the position

of the erosion front as function of time (for constant k_A) is

$$L = L_0 - \frac{k_A}{\bar{\rho}} t \tag{3}$$

This equation is valid for $0 \le t \le t_A$, where t_A is the time required for all of the A phase (the fast-eroding phase) to erode. This is the time at which the erosion front reaches the center of the tablet. This time constant t_A can be calculated by setting $L = 0$ in Eq. 3

$$t_A \equiv \frac{L_0 \bar{\rho}}{k_A} \tag{4}$$

Integrating Eq. 1, the mass of A lost during erosion of the A domains is

$$m_A = M_A S \phi_{A0} (1 - p) k_A t \tag{5}$$

The corresponding transport equation that describes the release of species B from the A domains is

$$m_B = M_B S \phi_{A0} p k_A t \tag{6}$$

Analogous to the model equations for the fast eroding zone, transport equations can be written for the slowly eroding zone, considering a zero-order reaction for the degradation of B. In this case, the disappearance of the A domains and the shrinking of the B domains induces a change in the B surface area exposed to the buffer; therefore, the porosity of the tablet $\epsilon(x,t)$ continuously varies with both time and position (that is, along the tablet thickness). To model the porosity, a mass balance for species B in a differential element dx positioned at distance x from the center of the tablet is written

$$\epsilon(x, t) = \phi_{A0} + \int_{\frac{(L_o - x)\cdot\bar{\rho}}{K_A}}^{t - \frac{(L_0 - x)\cdot\bar{\rho}}{k_A}} \frac{k_B M_B}{\rho_B} \sigma(x, t') \cdot dt' \tag{7}$$

Here, k_B is the surface erosion rate associated with the scission of B-B bonds and dissolution of the B monomer and $\sigma(x,t)$ represents the surface area of B in contact with the buffer per unit volume. To find an expression for $\sigma(x,t)$, the B phase is modeled as spheres with an average diameter d_0 (note that this is a surface-area average) for each infinitesimal volume Sdx. It is important to recognize that these spheres could be interconnected or disconnected. If they are interconnected, the device retains its mechanical integrity; if not, the spheres erode away into the surrounding buffer, which acts as an infinite medium and degrade. Then, $\sigma(x,t)$ becomes a function of time through the cube root of the porosity and is given by (for spherical domains $\sigma = 6/d$ and $d/d_0 = ((1 - \epsilon)/\phi_{B0})^{1/3}$, where subscript 0 indicates initial condition).

$$\sigma(x, t) \equiv \frac{6}{d_0} (1 - \epsilon)^{-1/3} \phi_{B0}^{1/3} \tag{8}$$

Applying the Leibniz rule to integrate Eq. 7 and imposing the condition that, at time $t = 0+$, the porosity in the infinitesimal volume Sdx is equal to the volume fraction of A domains, we obtain an analytical expression for the porosity $\epsilon(x,t)$

$$\epsilon(x, t) = 1 - \phi_{B0} \left[1 - \alpha \left(t - \frac{(L_0 - x)\bar{\rho}}{k_A} \right) \right]^3 \tag{9}$$

It is important to note that the functionality for ϵ with respect to the spatial dimension x is obtained considering that A domains between $x = L_0$ and the surface at x must completely degrade for the surface at x to be exposed to the water. Here, α is defined as

$$\alpha \equiv \frac{2 k_B M_B}{d_0 \rho_B} \tag{10}$$

The term α represents a time constant for the degradation of phase B with dimensions of reciprocal time. As a consequence, Eq. 9 is valid for values of x and t such that ϵ is always greater than zero. In other words, the B domains present in each of the infinitesimal volumes of the tablet erode after being in contact with water for a time equal to t_B. Additionally, t_B can be viewed as the time at which the tablet starts to shrink, that is, when $x = L_0$, the time at which $\epsilon = 1$ is t_B and is given by $t_B = 1/\alpha$. Thus, the total time required for the complete erosion of the tablet is the sum of the two time constants, t_A and t_B.

It is instructive to recognize that the condition $t_A > t_B$ could also occur in the systems under consideration. For this condition to occur, d_0 must be decreased or L_0 must be increased. Decreasing d_0 causes the spherical domains to be unconnected, thus compromising the mechanical integrity of the device; increasing L_0 may violate the assumptions of no diffusion control and 1-D transport; hence, this case is not considered here. Thus, t_A is always less than t_B in this work.

Results and Discussion

When $t_A < t_B$, three different regimes $[0, t_A]$ $[t_A, t_B]$ $[t_B, t_A + t_B]$ may be distinguished. For each of these regimes, the mass of B eroded can be calculated by integration with respect to position ($x \in [0, L_0]$) and time ($t \in [0, t]$) of the mass balance of B species in B domains

$$m_B = \frac{\beta t}{3\alpha} - \frac{\beta}{12\alpha^2} \left[1 - (1 - \alpha t)^4 \right] \qquad t \le t_A \tag{11}$$

$$m_B = \frac{\beta t_A}{3\alpha} - \frac{\beta}{12\alpha^2} \left[(1 - \alpha(t - t_A))^4 - (1 - \alpha t)^4 \right] \qquad t_A \le t \le t_B \tag{12}$$

$$m_B = \frac{\beta t_A}{3\alpha} - \frac{\beta}{12\alpha^2} (1 - \alpha(t - t_A))^4 \qquad t_B \le t \le t_B + t_A \tag{13}$$

$$\beta = \frac{6 k_B \phi_{B0} M_B S k_A}{d_0 \bar{\rho}} \tag{14}$$

Adding the mass of B lost from the A domains and normalizing with respect to the initial mass of B in the tablet, the mass fraction of B eroded can be obtained. Finally, the mass fractions of A (x_A) and B monomer (x_B) released from the tablet during the three regimes are

$$x_A = \frac{m_A}{m_{A0}} = \frac{t}{t_A} \qquad t \le t_A \tag{15}$$

$$x_B = \frac{m_B}{m_{B0}} = \frac{t}{t_A} - \delta \cdot \left[1 - (1 - \alpha t)^4\right] \qquad t \le t_A \tag{16}$$

$$x_B = \frac{m_B}{m_{B0}} = 1 - \delta \cdot \left[(1 - \alpha(t - t_A))^4 - (1 - \alpha t)^4\right] \qquad t_A \le t \le t_B \tag{17}$$

$$x_B = \frac{m_B}{m_{B0}} = 1 - \delta \cdot (1 - \alpha(t - t_A))^4 \qquad t_B \le t \le t_B + t_A \tag{18}$$

$$\delta = \frac{\beta}{12\alpha^2} \tag{19}$$

From the above equations, it is clear that in the first regime, the erosion rate of B increases with the exposed surface and reaches a maximum by the time all of the A is eroded. In the second regime, the erosion rate of B decreases as consequence of the decreasing exposed surface; and, at the end, in the third regime the mass fraction of B eroded approaches unity with zero slope.

p(CPP-SA) and p(CPH-SA) 20:80 erosion

Equations 15–18 can be used to fit monomer release data from p(CPP-SA) 20:80 (or p(CPH-SA) 20:80) copolymers. From the fit of Eq. 15 to SA release data, the SA erosion rate k_A can be obtained. Once k_A is obtained, t_A can be calculated using Eq. 4. Knowing t_A, the fit of Eq. 16 to CPP (or CPH) release data in the first regime ($t \le t_A$) can be used to obtain the CPP (or CPH) erosion rate k_B. Once both k_A and k_B are known, the CPH release profiles in regimes 2 and 3 can be predicted by the model using Eqs. 17 and 18. The parameters that are known in this analysis are L_0, d_0, p, ρ_A, ρ_B, M_A, M_B, and the copolymer composition. From AFM experiments (Shen et al., 2001), the value of d_0 is estimated to be of the order of 25 nm. The value of p has been chosen to be 0.07 based on image analysis of the surface fraction of SA and CPH domains in the AFM experiments of Shen et al. (2001b). The density values have been taken from Mathiowitz et al. (1990b). The values of these parameters for the two experimental systems considered below are shown in Table 1.

A combination of UV-Vis spectrophotometry and high-pressure liquid chromatography (Tamada and Langer, 1990) can be used to measure the release of the individual monomers, SA and CPP (or CPH). Using these methods, Tamada and Langer (1992, 1990) have obtained release data for SA and CPP release from p(CPP-SA) 20:80 copolymer tablets degrading in phosphate buffered saline solution (pH = 7.4) at 37°C. The SA release data (open circles) is fit with Eq. 15 and is shown in Figure 4. The value of k_A obtained from this fit is 1.1×10^{-4} mol/cm^2 day. Using this value of k_A, t_A for this system is calculated from Eq. 4 as 3.3 days.

Table 1. Model Parameters Determined by Experiments

Parameter	Value
L_0	0.075 cm
d_0	25 nm
p	0.07
ρ_A	1.1 g/cm^3
ρ_B	1.1 g/cm^3
M_A	182
$M_{B,\,\mathrm{CPH}}$	342
$M_{B,\,\mathrm{CPP}}$	300

The CPP release data (open squares) for $t \le 3.3$ days is fit with Eq. 16, and is also shown in Figure 4. The value of k_B obtained from this fit is 2.2×10^{-9} mol/cm^2 day. As expected, the SA erosion rate is much higher (~ 5 orders of magnitude) than the CPP erosion rate. It is instructive to note here that k_A represents the erosion rate of both SA-SA and SA-CPP bonds. Using the values of k_B just obtained, the value of t_B can be calculated using $t_B = 1/\alpha$, and for this system, $t_B = 8.4$ days. Thus, the total time required for erosion of the CPP domains should be $t_A + t_B = 11.7$ days. In addition, the CPP release for regimes 2 and 3 can be *predicted* using Eqs. 17 and 18. These predictions are compared to the experimental release data in Figure 4 and, as shown, the agreement is excellent. It is important to note that the theoretical CPP release profiles in regimes 2 and 3 and the total CPP release time are predicted from the model once k_A and k_B are known.

We have extended the method developed by Tamada and Langer to monitor individual release of SA and CPH monomer from tablets of p(CPH-SA) 20:80 copolymers (Shen et al., 2002). The details of the experimental techniques are described elsewhere (Shen et al., 2002). The theoretical fits of individual monomer release from the current model and the experimental data are shown in Figure 5. The value of k_A obtained from this fit (using Eq. 15) is 2.2×10^{-4} mol/cm^2 day. Using this value of k_A, t_A for this system is calculated

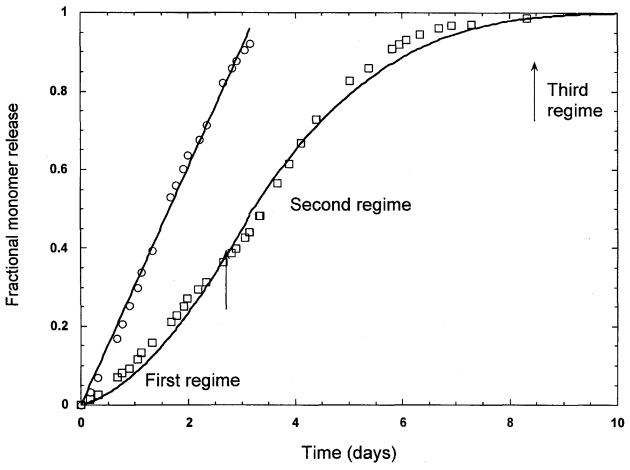

Figure 4. Experimental results vs. model for the erosion of *p*(CPP-SA) 20:80 tablets (Tamada and Langer, 1990).

CPP = □, SA = ○. The solid lines represent model fits to monomer release (Eqs. 15–18).

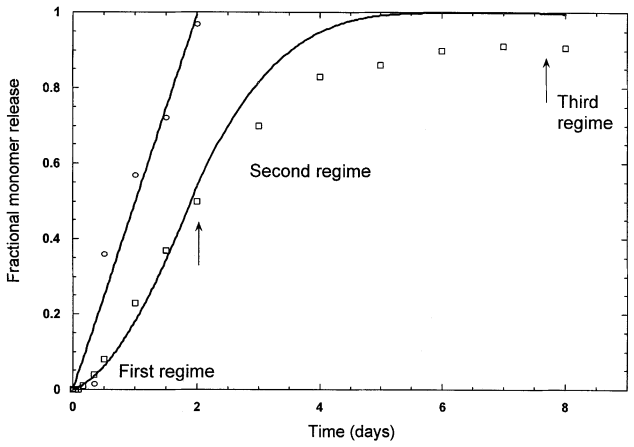

Figure 5. Experimental results vs. model for the erosion of *p*(CPH-SA) 20:80 tablets (Shen et al., 2001a).

CPH = □, SA = ○. The solid lines represent model fits to monomer release (Eqs. 15–18).

from Eq. 3 as 2.0 days. It is instructive to note that the value of k_A obtained from this fit is of the same order of magnitude as that obtained from the SA released in the p(CPP-SA) 20:80 system (see Table 2 for a summary of the calculated parameters of the p(CPP-SA) 20:80 and p(CPH-SA) 20:80 systems). The CPH release data (open squares) for $t \leq 2.0$ days is fit with Eq. 16 and is also shown in Figure 5. The value of k_B obtained from this fit is 5.2×10^{-10} mol/cm^2 day. Once again, the SA erosion rate is much higher (>5 orders of magnitude) than the CPP erosion rate. In addition, the CPH erosion rate is slower than the CPP erosion rate (see Table 2). This is expected since CPH is more hydrophobic than CPP (see Figure 1). Using the value of k_B just obtained, the value of t_B can be calculated using $t_B = 1/\alpha$, and for the CPH-SA system, $t_B = 7.7$ days. Thus, the total time required for erosion of the CPH domains should be $t_A + t_B = 9.7$ days. In addition, the CPH release for regimes 2 and 3 can be predicted using Eqs. 17 and 18. These predictions are compared to the experimental release data in Figure 5 and, as shown, the model correctly predicts the shape of the release profile. However, the model overpredicts the CPH release in the second and third regimes. The reasons for this discrepancy are discussed later.

Using the values of k_A and k_B, the porosity ϵ in the CPH-SA system can be plotted as a function of both position and time using Eq. 9. This porosity profile is shown in Figure 6. As expected, ϵ approaches 1 at the surface ($x = L_0$) at $t = t_A$.

Drug release from p(CPH-SA) 20:80

Based on experimental data of drug release from polyanhydrides with microphase separation (such as p(CPH-SA) 20:80), we have proposed that the compatibility of the polymer and drug drives the thermodynamic partitioning of the drug within the microdomains of the polymer (Shen et al., 2001a). Heterogeneous polymers such as p(CPH-SA) 20:80 and 80:20 provide a microphase-separated environment in which the drug can preferentially partition itself. Drug molecules loaded into such polymers will attempt to distribute themselves into

Table 2. Model Parameters from Fits to Experimental Monomer Release Data

Parameter	p(CPP-SA) 20:80	p(CPH-SA) 20:80
k_A	1.1×10^{-4} mol/cm^2 day	2.2×10^{-4} mol/cm^2 day
t_A	3.3 days	2.0 days
k_B	2.2×10^{-9} mol/cm^2 day	5.2×10^{-10} mol/cm^2 day
t_B	8.4 days	7.7 days

compatible regions until saturation is reached. If very few compatible domains are present, the excess drug will be forced to distribute itself into less compatible regions, resulting in a pronounced burst effect. Drug solubility also plays a key role in determining the release profile characteristics from bioerodible polymers. In heterogeneous systems, the drug preferentially partitions itself into compatible domains. Once these domains become saturated, the drug attempts to solubilize within the less compatible regions. Any excess drug precipitates out, resulting in an initial burst.

An example of a solute exhibiting this partitioning behavior is *p*-nitroaniline (PNA), for which experimental evidence points to the preferential partitioning within the aromatic-rich (CPP- or CPH-rich) domains in p(CPP-SA) or p(CPH-SA) 20:80 copolymers (Mathiowitz and Langer, 1987; Shen et al., 2002). Thus, we define a partition coefficient P as the ratio of drug concentration in the B (CPP or CPH) phase to that in the A (SA) phase. The excess drug in the system is released in the form of a burst. It is important to understand that the amount of drug released in the burst is the sum of the amounts released from both phases. However, the model in its current form does not distinguish between the drug released during the burst from either phase. Thus, the drug released during the burst is treated only as a consequence of the supersaturation in the polymer. It can be proved that the fraction of drug released x_D is given by

$$x_D = (1-b)x_{D,p} + b \tag{20}$$

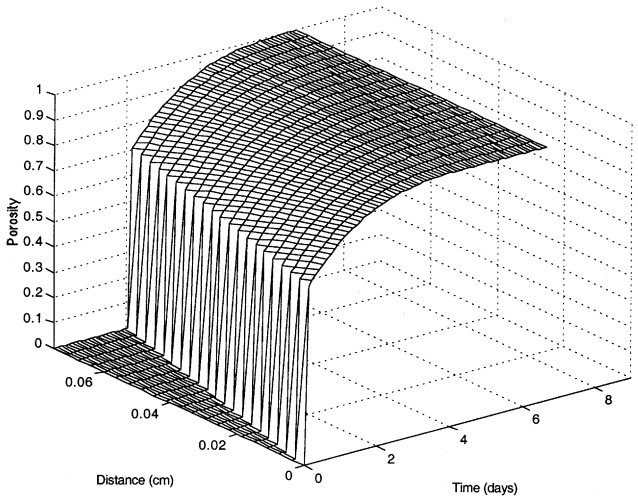

Figure 6. Porosity distribution within *p*(CPH-SA) 20:80 tablet as a function of position and time (Eq. 9).

Here, b is the fraction of drug released in the burst and $x_{D,p}$ is the fraction of drug released that is partitioned within the polymer. The total mass of drug released that is partitioned within the microdomains of the polymer is given by

$$m_{D,p} = x_A \phi_{A0} S L_0 C_{D,A0} + x'_B \phi_{B0} S L_0 C_{D,B0} \qquad (21)$$

Here x_A is the mass fraction of A released (given by Eq. 15), x'_B is the mass fraction of B released from the B phase (given by subtracting Eq. 6 from Eq. 11 and normalizing with respect to the total mass of the B phase), $C_{D,A0}$ is the initial concentration of drug in the A phase, and $C_{D,B0}$ is the initial concentration of drug in the B phase. The initial mass of drug that is partitioned within the two phases is

$$m_{D0} = (\phi_{A0} C_{D,A0} + \phi_{B0} C_{D,B0}) S L_0 \qquad (22)$$

Using the definition of the partition coefficient, dividing Eq. 21 by Eq. 22, and using Eq. 20, the fractional drug released from the p(CPH-SA) 20:80 polymer can be derived as

$$x_D = (1-b)\frac{(x_A \phi_{A0} + x'_B \phi_{B0} P)}{\phi_{A0} + \phi_{B0} P} + b \qquad (23)$$

The burst is modeled as the fraction of drug released in the early stages of release by comparison with the experimental data. Then, the drug release data can be fit to Eq. 23 in each regime of release and P, the partition coefficient, can be estimated by fitting Eq. 23 to the first regime. In addition, since experimental data for monomer release from drug-loaded polyanhydrides is available, the monomer release rate constants k_A and k_B can also be estimated using the method described earlier.

Figure 7 shows the release of SA, CPH, and PNA from a p(CPH-SA) 20:80 copolymer containing 10% w/w of PNA. The drug-containing copolymer is in the form of a 110 mg tablet with a diameter of 10 mm and a thickness of 1.5 mm. The SA release is fitted to Eq. 15 and the value of k_A that is obtained from the fit is 1.9×10^{-4} mol/cm^2 day. This value is relatively unchanged from the value of k_A obtained when no PNA is present (see Table 2). This suggests that the presence of PNA does not affect the release of SA or, in other words, PNA does not interact strongly with SA in p(CPH-SA) 20:80. The CPH release during the first regime ($t \le 2.3$ days) is fitted to Eq. 16, and the value of k_B obtained from the fit is 1.1×10^{-9} mol/cm^2 day. This value is about five times the value of k_B when no PNA is present (see Table 2). This suggests that the presence of PNA affects the release of CPH; it accelerates the rate of release of CPH. As before, the CPH release in regimes 2 and 3 is predicted using the value of k_B obtained from the fit of the data in the first regime to the model.

By observation of the PNA release data (filled circles) in Figure 7, the value of b is estimated as 0.41. Using Eq. 23, the value of P is estimated from the PNA release data in the first regime ($t \le 2.3$ days) as 2.55. This value of P indicates that the PNA is 2.55 times more soluble in the CPH phase as it is in the SA phase; thus, the model shows that the PNA partitions into the CPH phase in the p(CPH-SA) 20:80 copolymer. This result from the model is in agreement with several experimental studies (Mathiowitz and Langer, 1987; Shen et al., 2001a) of PNA release from p(CPP-SA) 20:80 copolymers that suggest PNA affinity to CPH.

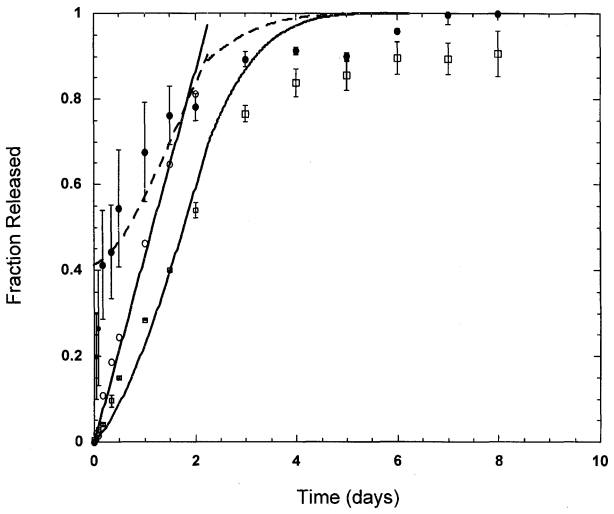

Figure 7. Experimental results vs. model for the individual monomer (CPH = □, SA = ○) and PNA (●) release from *p*(CPH-SA) 20:80 tablets.

The solid lines represent model fits to monomer release (Eqs. 15–18) and the dotted line represents the model fit to PNA release (Eq. 23).

p(CPH-SA) 80:20 erosion

As stated earlier, the p(CPH-SA) and p(CPP-SA) systems exhibit microphase separation when one component is present in excess of 80 mol %. The preceding discussion was concerned with the case for which the fast eroding component A was present in excess of 80 mol %. Now, the analysis is extended to the situation when the slowly eroding component B is present in excess of 80 mol %. In the former case, it was assumed that the fraction of A within the B domains is negligible; here, we assume that there is no B within the A domains, that is, $p = 0$. Once again, the basis of this assumption is the AFM data in Shen et al. (2001b).

In this case, the disappearance of the A domains and the growth of the B domains induces a change in the B surface area exposed to the buffer; therefore, the porosity of the tablet $\epsilon(x,t)$ continuously varies with both time and position (that is, along the tablet thickness). As before, a mass balance for species B in a differential element dx, positioned at distance x from the center of the tablet, is written (see Eq. 7 for the integral form). To find an expression for $\sigma(x,t)$, the surface area of B in contact with the buffer per unit volume, the A phase is modeled as spheres with a (surface-area average) diameter d_0, for each infinitesimal volume Sdx. Then, $\sigma(x,t)$ becomes a function of the porosity ϵ and is given by

$$\sigma = \frac{6\phi_{A0}^{1/3}}{d_0}\epsilon^{2/3}(1-\epsilon) \qquad (24)$$

The factor $(1-\epsilon)$ accounts for the decrease in surface area as the microdomains coalesce. Substituting Eq. 24 in Eq. 7,

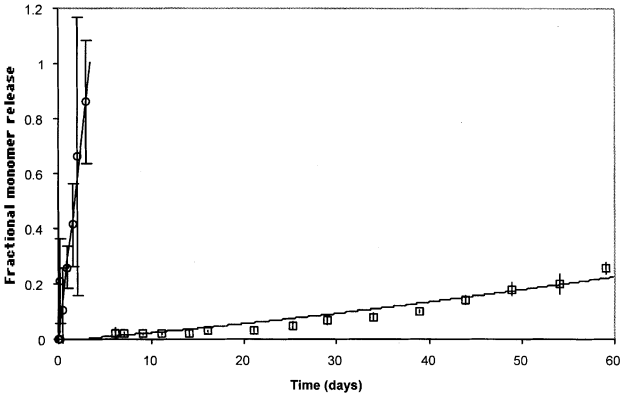

Figure 8. Experimental results vs. model for the erosion of *p*(CPH-SA) 80:20 tablets (Shen et al., 2001a).

CPH = □, SA = ○. The solid lines represent model fits to monomer release (Eqs. 15 and 26).

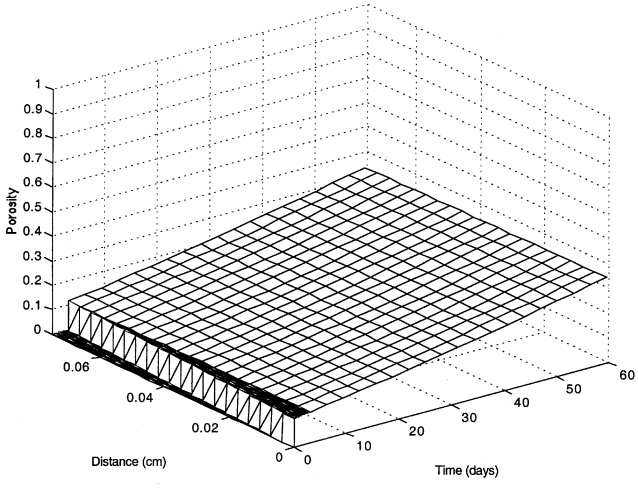

Figure 9. Porosity distribution within (CPH-SA) 80:20 tablet as a function of position and time (obtained from integration of Eq. 25).

we obtain an ordinary differential equation for the porosity $\epsilon(x,t)$ given by

$$\frac{d\epsilon}{dt} = -\frac{6k_B M_B \phi_{A0}^{2/3}}{d_0 \rho_B}\epsilon^{2/3}(1-\epsilon) \tag{25}$$

The porosity can be obtained via numerical integration of Eq. 25 once k_A and k_B are known. The expression for the mass of A released is given by Eq. 11. This release of A induces porosity in the p(CPH-SA) 80:20 polymer and, thus, the mass of B released as a function of time is given by

$$m_B = \int_0^t M_B(1-p)(\epsilon - \phi_{A0})Sk_A dt' \tag{26}$$

The total mass of B released is normalized with respect to the initial mass of B in the system to obtain the fraction of B released as a function of time. We have obtained experimental data for SA and CPH release from p(CPH-SA) 80:20 tablets (Shen et al., 2002). This data and the model fits are shown in Figure 8. From the fit of the SA release data, the value of k_A is obtained as 1.4×10^{-4} mol/cm^2 day. This value is of the same order of magnitude as the value obtained for the p(CPH-SA) 20:80 copolymer, which is expected since k_A describes the rate of scission of SA-SA bonds and subsequent dissolution of the SA monomer. Also shown in Figure 8 is the fit of the CPH release data for a period of 60 days. During this period, about 30% of the CPH was released. The value of k_B obtained from the fit is 8.0×10^{-11} mol/cm^2 day. This value is about six times slower than the value of k_B obtained for CPH release from p(CPH-SA) 20:80, suggesting that there are attributes of the microstructure in the 80:20 case that are different from that of the 20:80 case. This discrepancy is discussed in the next section.

Using the values of k_A and k_B, the porosity ϵ in the p(CPH-SA) system can be plotted as a function of both position and time. This porosity profile for the first 60 days of release is shown in Figure 9. It is instructive to note that ϵ approaches ~ 0.33 after about 60 days of release in reasonable agreement with $\sim 30\%$ of CPH released after the same time.

Limitations of the model

The model assumes that k_A and k_B are the rates at which monomers are produced as reaction products when the polymer is exposed to buffer. In reality, when the polymer is exposed to buffer solution, the degradation process that takes place is probabilistic and leads to products with a distribution of chain lengths. In other words, oligomeric species are first produced before monomer is released. This explains the overprediction observed in Figures 5 and 7. On the other hand, the model appears to work well for the CPP release from p(CPP-SA) 20:80. This indicates that apart from the distribution of chain lengths, k_A and k_B must depend on other factors. This is discussed next.

It is well known (Mathiowitz et al., 1990b) that both the p(CPP-SA) and the p(CPH-SA) systems are semicrystalline. It has also been shown that monomer crystals form during erosion (Goepferich and Langer, 1993). The model does not explicitly treat the effects of crystallinity on erosion. This may also explain the differences between the value of k_B obtained for p(CPH-SA) 20:80 and 80:20. It has been shown by Mader et al. (1997) that the local pH during erosion of p(CPP-SA) decreases, leading to increased solubility of the degradation products, and, thus, accelerated erosion. We argue that this increase in solubility is compensated for by the formation of monomer crystals during degradation, thus canceling the effect of both phenomena. This effect may be less pronounced in the p(CPH-SA) case since CPH is less crystalline than CPP and degrades much more slowly (Mathiowitz et al., 1990b; McCann et al., 1999).

Another factor that limits the model is the absence of any molecular weight and/or polydispersity dependence of the rate constants. The number average molecular weights for the p(CPH-SA) 20:80 and 80:20 used in the experiments that the model is fitted to are 8,800 and 5,500, respectively (Shen et

al., 2001). New expressions for k_A and k_B need to be developed that account for the statistical distribution of chain lengths, degree of crystallinity, the local pH, and polymer molecular weight.

Other aspects that currently limit the model include the lack of reliable data for the parameters d_0 and p and the absence of polymer-drug interactions. These parameters have been estimated by comparison to AFM data obtained on the CPH-SA system, but more detail on the solid-state microstructure of the copolymers is needed to correctly estimate these parameters. As seen in the data of Figure 7, the presence of the drug influences the degradation rate, suggesting the presence of polymer-drug interactions. The model "lumps" these interactions within the partition coefficient P, but a more thorough understanding of the nature of the interactions and their effect on the monomer release is needed. Further, a more detailed argument for the burst effect needs to be developed. Refinements of the current model based on these considerations are underway.

Conclusions

A new model was developed to understand the mechanism of degradation and drug release kinetics of surface-erodible polymers. This model takes into account the phenomenon of microphase separation that has been observed for polyanhydrides of certain copolymer compositions. The model assumes that erosion is dominated by degradation and, thus, in a system with a fast eroding and a slow eroding species, two rate constants, one for each species, essentially control the evolution of the polymer microstructure. Expressions were derived for the fraction of each monomer released, as well as for the porosity in the system. When drugs are loaded into such heterogeneous polymers, they undergo thermodynamic partitioning depending upon their compatibility with each phase of the copolymer. This aspect has been modeled via a partition coefficient. The solutions of the model equations were fitted to experimental data on monomer release kinetics from two polyanhydride systems to obtain the erosion rate constants. Drug release kinetics experiments were compared to the model solution for drug release and the partition coefficient of the drug is obtained from the fits. The comparisons to the data are promising, while pointing out the limitations of the model. The model does not account for oligomer formation prior to monomer release or for the dependence of the rate constants on parameters such as the degree of crystallinity, the local pH, and the polymer molecular weight. These limitations will be addressed in a future publication.

Acknowledgments

The authors acknowledge financial support from the Whitaker Foundation, the ISU Office of Biotechnology, and the PRIN Research Program (1999-2001) in Industrial and Information Engineering of the Italian Ministry for University and Scientific and Technological Research (MURST). We also thank Elizabeth Shen for providing the CPH-SA and PNA release data.

Literature Cited

Batycky, R. P., J. Hanes, R. Langer, and D. A. Edwards, "A Theoretical Model of Erosion and Macromolecular Drug Release from Biodegrading Microspheres," *J. Pharm. Sci.*, **86**, 1464 (1997).

Chasin, M., D. Lewis, and R. Langer, "Polyanhydrides for Controlled Drug Delivery," *Biopharm. Mfg.*, 33 (Feb. 1988).

Chickering, D., J. Jacob, and E. Mathiowitz, "Poly(fumaric-co-sebacic) Microspheres as Oral Drug Delivery Systems," *Biotech. Bioeng.*, **52**, 96 (1996).

Dang, W., T. Daviau, P. Ying, Y. Zhao, D. Nowotnik, C. Clow, B. Tyler, and H. Brem, "Effects of GLIADEL Wafer Initial Molecular Weight on the Erosion of Wafer and Release of BCNU," *J. Contr. Rel.*, **42**, 83 (1996).

Domb, A. J., and R. Langer, "Polyanhydrides: I. Preparation of High Molecular Weight Polyanhydrides," *J. Polym. Sci., Polym. Chem. Ed.*, **25**, 3373 (1987).

Goepferich, A., "Mechanisms of Polymer Degradation," *Biomaterials*, **17**, 103 (1996a).

Goepferich, A., "Polymer Degradation and Erosion: Mechanisms and Applications," *Eur. J. Pharm. Biopharm.*, **42**, 1 (1996b).

Goepferich, A., and R. Langer, "Modeling of Polymer Erosion," *Macromolecules*, **26**, 4105 (1993).

Goepferich, A., and R. Langer, "Modeling of Monomer Release from Bioerodible Polymers," *J. Contr. Rel.*, **33**, 55 (1995).

Goepferich, A., L. Shieh, and R. Langer, "Aspects of Polymer Erosion," *Mat. Res. Soc. Symp. Proc.*, **394**, 155 (1995).

Heatley, F., M. Humadi, R. Law, and A. D'Emanuele, "Erosion of a 1,3-bis(p-carboxyphenoxy)propane-sebacic Acid Poly(anhydride) Copolymer by Water Vapor Studied by ^{1}H and ^{13}C Solid-State NMR Spectroscopy," *Macromolecules*, **31**, 3832 (1998).

Kuntz, R., and W. M. Saltzman, "Polymeric Controlled Delivery for Immunization," *Tibtech*, **15**, 364 (1997).

Langer, R., "New Methods of Drug Delivery," *Science*, **249**, 1527 (1990).

Leong, K., P. D'Amore, M. Marletta, and R. Langer, "Bioerodible Polyanhydrides as Drug-Carrier Matrices. II. Biocompatibility and Chemical Reactivity," *J. Biomed. Mat. Res.*, **20**, 51 (1986).

Leong, K. W., B. C. Brott, and R. Langer, "Bioerodible Polyanhydrides as Drug-Carrier Matrices. I: Characterization, Degradation, and Release Characteristics," *J. Biomed. Mat. Res.*, **19**, 941 (1985).

Mader, K., S. Nitschke, R. Stosser, H.-H. Borchert, and A. Domb, "Non-Destructive and Localized Assessment of Acidic Microenvironments inside Biodegradable Polyanhydrides by Spectral Spatial Paramagnetic Resonance Imaging." *Polymer*, **38**, 4785 (1997).

Mathiowitz, E., C. Amato, and R. Langer, "Polyanhydride Microspheres: 3. Morphology and Characterization of Systems made by Solvent Removal," *Polymer*, **31**, 547 (1990a).

Mathiowitz, E., H. Bernstein, S. Giannos, P. Dor, T. Turek, and R. Langer, "Polyanhydride Microspheres. IV. Morphology and Characterization of Systems made by Spray Drying," *J. Appl. Polym. Sci.*, **45**, 125 (1992).

Mathiowitz, E., and R. Langer, "Polyanhydride Microspheres as Drug Carriers. I. Hot-Melt Microencapsulation," *J. Contr. Rel.*, **5**, 13 (1987).

Mathiowitz, E., E. Ron, G. Mathiowitz, C. Amato, and R. Langer, "Morphological Characterization of Bioerodible Polymers: 1. Crystallinity of Polyanhydride Copolymers," *Macromolecules*, **23**, 3212 (1990b).

Mathiowitz, E., W. M. Saltzman, A. Domb, and R. Langer, "Polyanhydride Microspheres as Drug Carriers. II. Microencapsulation by Solvent Removal," *J. Appl. Polym. Sci.*, **35**, 755 (1988).

McCann, D. L., F. Heatley, and A. D'Emanuele, "Characterization of Chemical Structure and Morphology of Eroding Polyanhydride Copolymer by Liquid-State and Solid-State 1H n.m.r.," *Polymer*, **40**, 2151 (1999).

Olivi, A., M. Ewand, T. Utsuki, B. Tyler, A. Domb, D. Brat, and H. Brem, "Interstitial Delivery of Carboplatin via Biodegradable Polymers is Effective Against Experimental Glioma in the Rat," *Cancer Chemother. Pharmacol.*, **39**, 90 (1996).

Park, E., M. Maniar, and J. Shah, "Influence of Physicochemical Properties of Model Compounds on their Release from Biodegradable Polyanhydride Devices," *J. Contr. Rel.*, **48**, 67 (1997).

Park, E., M. Maniar, and J. Shah, "Biodegradable Polyanhydride Devices of Cefazolin Sodium, Bupivacaine, and Taxol for Local Drug Delivery: Preparation, and Kinetics and Mechanism of in Vitro Release," *J. Contr. Rel.*, **52**, 179 (1998).

Peppas, N. A., and R. Langer, "New Challenges in Biomaterials," *Science*, **263**, 1715 (1994).

Ron, E., E. Mathiowitz, G. Mathiowitz, A. Domb, and R. Langer, "NMR Characterization of Erodible Copolymers," *Macromolecules*, **24**, 2278 (1991).
Shen, E., M. Kipper, B. Dziadul, M.-K. Lim, and B. Narasimhan, "Mechanistic Relationships between Polymer Microstructure and Drug Release Kinetics in Bioerodible Polyanhydrides," *J. Contr. Rel.*, **82**, 115 (2002).
Shen, E., R. Pizsczek, B. Dziadul, and B. Narasimhan, "Microphase Separation in Bioerodible Copolymers for Drug Delivery," *Biomaterials*, **22**, 201 (2001).
Shieh, L., J. Tamada, Y. Tabata, A. Domb, and R. Langer, "Drug Release from a New Family of Biodegradable Polyanhydrides," *J. Contr. Rel.*, **29**, 73 (1994).
Tamada, J., and R. Langer, "Review: The Development of Polyanhydrides for Drug Delivery Applications," *J. Biomater. Sci., Polymer Ed.*, **3**, 315 (1992).
Tamada, J. A., and R. S. Langer, "Mechanism of the Erosion of Polyanhydride Drug Delivery Systems," *Proceed. Intern. Symp. Control. Rel. Bioact. Mater.*, **17**, 156 (1990).
Thombre, A. G., and K. J. Himmelstein, "Modeling of Drug Release Kinetics from a Laminated Device having an Erodible Drug Reservoir," *Biomaterials*, **5**, 250 (1984).
Thombre, A. G., and K. J. Himmelstein, "A Simultaneous Transport-Reaction Model for Controlled Drug Delivery from Catalyzed Bioerodible Polymer Matrices," *AIChE J.*, **31**, 759 (1985).
Varelas, C. G., D. G. Dixon, and C. A. Steiner, "Mathematical Model of Mass Transport through Dispersed-Phase Polymer Networks," *AIChE J.*, **41**, 805 (1995a).
Varelas, C. G., D. G. Dixon, and C. A. Steiner, "Zero-Order Release from Biphasic Polymer Hydrogels," *J. Contr. Rel.*, **34**, 185 (1995b).
Zygourakis, K., "Development and Temporal Evolution of Erosion Fronts in Bioerodible Controlled Release Devices," *Chem. Eng. Sci.*, **45**, 2359 (1990).
Zygourakis, K., and P. A. Markenscoff, "Computer-Aided Design of Bioerodible Devices with Optimal Release Characteristics: a Cellular Automata Approach," *Biomaterials*, **17**, 125 (1996).

Manuscript received Dec. 17, 2001, and revision received May 9, 2002.